

PERSPECTIVE ARTICLE

Design of customized soft-tissue substitutes for posterior single-tooth defects: A proof-of-concept in-vitro study

Yue Sun^{1,2}  | Tao Yu^{3,2,5} | Malin Strasdning² | Xinran Liu^{3,2,5} | Felix Burkhardt² | Birgit Schäfer⁴ | Irena Sailer²  | Dobrila Nestic² 

¹Division of Orthodontics, Beijing Stomatological Hospital, Capital Medical University, Beijing, China

²Division of Fixed Prosthodontics and Biomaterials, University Clinic of Dental Medicine, University of Geneva, Geneva, Switzerland

³Clinical Division, Peking University Hospital of Stomatology, Beijing, China

⁴Geistlich Pharma AG, Wolhusen, Switzerland

⁵National Engineering Laboratory for Digital and Material Technology of Stomatology, Beijing Key Laboratory of Digital Stomatology, Beijing, China

Correspondence

Dobrila Nestic, Division of Fixed Prosthodontics and Biomaterials, University Clinic of Dental Medicine, University of Geneva, Rue Michel-Servet 1, CH-1211 Geneva 4, Switzerland.
Email: dobrila.nestic@unige.ch

Funding information

Geistlich Pharma AG

Abstract

Objectives: Soft-tissue volume augmentation treatments do not provide the satisfactory long-term functional and esthetic outcomes. The aim of the study was to develop a standardized digital procedure to design individual soft-tissue substitutes (STS) and apply mathematical modeling to obtain average shape STS for single posterior tooth defects.

Material and methods: Thirty-three casts from 30 patients were scanned. STS were designed with a computer-aided design software and a systematic procedure standardized the measurements across all STS using 3D-analysis software. The occlusal, mesial–distal, and buccal–lingual planes were defined to partition, each STS and produce a mesh. The thickness values of each 3D slice were documented in a coordinate system chart to generate a scatter graph. Graphs were embedded into images (Orange software) and images were analyzed via hierarchical clustering.

Results: Three STS groups were identified according to shape. Two shapes corresponded to the maxilla defects: a square ($n = 13$) with dimensions of 10 mm in a lingual–buccal (length) and 7–10 mm in a mesial–distal (width) direction; a rectangle ($n = 11$) of 11 mm in length and 4–7 mm in width. The average shape for mandible defects ($n = 9$) was smaller (6–8 mm in length, 5–10 mm in width). The highest thickness in all STS was in the buccal portion, above the alveolar ridge, with median values of 2 mm. The lowest thickness of 0.2 mm was at the edges.

Conclusions: The study developed novel methodology to design customized, as well as average shape STS for volume augmentation. Future STS harboring adapted geometry might increase volume augmentation efficiency and accuracy, while reducing surgical time.

KEYWORDS

biomaterial(s), CAD, digital imaging/radiology, gingiva, personalized medicine, prosthetic dentistry/prosthodontics

Yue Sun, Tao Yu contributed equally to this study.

This is an open access article under the terms of the Creative Commons Attribution-NonCommercial-NoDerivs License, which permits use and distribution in any medium, provided the original work is properly cited, the use is non-commercial and no modifications or adaptations are made.

© 2021 The Authors. *Clinical Oral Implants Research* published by John Wiley & Sons Ltd.

1 | INTRODUCTION

Tooth loss is inevitably associated with the decrease of soft- and hard-tissue volume over time (Van der Weijden et al., 2009). In addition to sufficient bone volume necessary for implant placement, the soft-tissue quality and quantity are crucial in maintaining long-term peri-implant health (Ackali et al., 2017; Gobbato et al., 2013). Tissue volume loss leads to biological and esthetic problems and often requires demanding functional and esthetic treatments prior to tooth- or implant-borne restorations. Importantly, insufficient amount of soft-tissue volume may lead to biological complications such as soft-tissue recession/dehiscence and crestal bone resorption (D. S. Thoma, Buranawat et al., 2014; Thoma, Muhlemann et al., 2014). To reduce the disadvantages of alveolar volume defects, soft-tissue augmentation is often performed prior to the prosthetic restoration (D. S. Thoma, Buranawat, et al., 2014). In case of tissue volume loss due to resorption processes, an increase of soft-tissue contours is indicated in order to stabilize and maintain peri-implant tissue health and improve esthetic outcomes (Sculean et al., 2019; D. S. Thoma et al., 2018).

The current gold standard for soft-tissue volume augmentation is the autogenous sub-epithelial connective tissue graft (CTG) (Basseti et al., 2016; D. S. Thoma, Buranawat, et al., 2014). CTG is mainly harvested from palatal or tuberosity areas (Amin et al., 2018; D. S. Thoma et al., 2018). This procedure has shown satisfying functional and esthetic outcomes, as well as clinically stable long-term results at pontic and implant sites (S. P. Bienz, Sailer, et al., 2017; De Bruyckere et al., 2015). However, several drawbacks are associated with this treatment approach: The surgery procedure is invasive as it creates a second wound and causes an increased patient discomfort

and morbidity (Cairo et al., 2017; Lorenzo et al., 2012; D. S. Thoma et al., 2016), the tissue availability is often limited due to the varying patient-related palate anatomy (Benninger et al., 2012), and the risk of infections is increased.

To provide an alternative for autogenous grafts, several soft-tissue substitutes (STS) were developed: allogenic, xenogenic, and synthetic (Toledano et al., 2020; Wolff et al., 2016). In addition to an unlimited availability and reduced patient morbidity, the use of off-shelf soft-tissue substitutes allows for a reduction of the intervention time (Cairo et al., 2017; Lorenzo et al., 2012; Sanz et al., 2009; D. S. Thoma, Buranawat, et al., 2014). However, all currently available STS are delivered as prefabricated, standard size blocks, and have to be customized according to the different 3D geometries of the individual defect sites, similar to CTG. The precision of trimming is operator-dependent, and the accuracy is nonoptimal. During the STS preparation time, the defect site is exposed, increasing the risk of infection and thus jeopardizing wound healing and the post-operative results. Hence, a reduction of the chair-side adjustments of the soft-tissue blocks would prove advantageous. To that end, STS need to be produced in shapes that would better correspond to individual edentulous defects and, therefore, either be ready for insertion without having to be shaped or require minimal chairside shape adjustments. While individualized STS still require more development, fabrication of a STS based on an average defect shape would allow easier handling for the surgeon, including preparation, insertion of the STS, and suturing.

The aim of this proof-of-concept study was to develop a standardized procedure for the digital designing of individual STS and a mathematical modeling tool to obtain average STS adapted to optimally fit single-tooth soft-tissue defects in the posterior jaw.

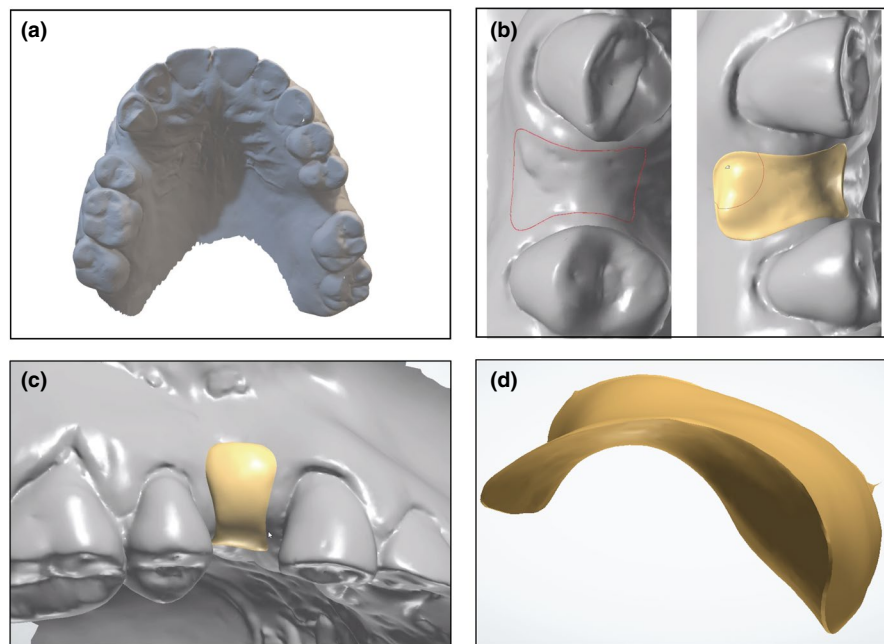


FIGURE 1 Design of the single STS. Imprint stone casts harboring a single posterior tooth defect were scanned with Imetric (a) and imported into the 3Shape software. The STS was outlined to optimally fit the defect, and the thickness was added by moving the mouse over the STS (b). Once the design of the STS was finished (c), the STL file was extracted for further analysis (d)

2 | MATERIALS AND METHODS

2.1 | Defect scans

Conventional stone casts from 30 patients with 33 single-tooth defects with two remaining natural neighboring teeth in the posterior region of maxilla and mandible were collected. Epidemiology studies indicate the high prevalence of loss of molar and premolar teeth in different world populations (Batista et al., 2012; Dye et al., 2019; Lin et al., 2001; Muller et al., 2007). The inclusion criterion was tooth extraction at least 6 months prior taking the impressions. Ethics approval was not required for this in vitro study. The 30 casts with 33 defect sites were scanned with a CAD/CAM laboratory scanner (Imetric4D; Courgenay; Switzerland), and STL files were generated (Figure 1A).

2.2 | Soft-tissue substitute (STS) design

To design an STS for volume augmentation, STL file of each scanned cast was imported into the software (3Shape dental designer Version19, 3Shape; Copenhagen; Denmark). The outline of the STS was designed according to the incision line, which was placed 1.5 mm away from the adjacent teeth to protect the papilla and extended 4 mm down to the vestibular side (Figure 1B). The shape and the thickness of each STS were adapted to optimally fill the defect on top of the residual tissue and, thus, achieve the desired final soft-tissue volume (Figure 1C). The designed STS together with the cast was exported as one entity into the software (Meshmixer Version 3.5, Autodesk) in order to extract the STS file from the cast file, while maintaining the same coordinate system (Figure 1D). The extracted STS was subsequently imported into the 3D analysis software (GOM Inspect) for further analysis.

2.3 | Soft-tissue substitute thickness measurements and clustering

GOM inspect was employed to measure the thickness across each designed STS. A systematic procedure was developed to standardize the measurements. First, the occlusal plane was defined based on three specific anatomical markers: the incisal point between the central incisors, and the mesial-palatal (for maxilla) or mesial-buccal (for mandible) cusps of the first molar (or a second molar in the case of a missing first molar) in each quadrant. Next, a mesial–distal plane was drawn through the centers of the adjacent teeth and perpendicular to the occlusal plane. The centers were defined at the viewing angle perpendicular to the occlusal plane based on the teeth adjacent to the defect as follows: (1) middle fossa for molars; (2) middle point between mesial fossa and distal fossa for upper molars; (3) buccal cusp for lower premolars; (4) middle point between cusp and cingulum for upper canine; (5) cusp for lower canine. A buccal–lingual plane was drawn through the mesial–distal central point of the

defect and perpendicular to both, occlusal plane and mesial–distal plane to obtain the planes in three dimensions (x,y,z) (Figure 2a). The point zero (0,0,0) was defined at the cross of mesial–distal plane, buccal–lingual plane, and the outer surface of the STS. Next, a buccal point was chosen at the cross of the buccal–lingual plane and the buccal margin of the STS. The same approach was applied to define the lingual point. The inner top point was defined as a point at the cross-curve of the inner surface and buccal–lingual plane, which was the farthest one relative to the line connecting the buccal and lingual points. A reference circle was thus obtained, connecting buccal, lingual, and inner top points. (Figure 2b). Radial sections were made starting from point zero. The number of sections at 1 mm distance depended on the circumference of the circle (Figure 2c). To measure the thickness in the mesial–distal direction, parallel sections were made from point 0.0.0 in the mesial and distal direction at 1 mm distance (Figure 2d). Each STS was thus divided into 3D slices where $x = 1$ mm, $y = 1$ mm and $z =$ thickness (Figure 3a). Individual thickness values of each slice for each STS were documented in an excel chart with a coordinate system where X-axis represented the buccal–lingual direction and Y-axis as the mesial–distal direction. To ensure reproducibility and accuracy, the thickness measurements were compared between two researchers for 14 STS. The observed differences were negligible (0.001 mm). Next, a scatter (“bubble”) graph was generated for each STS, where the circle depicted the thickness of each 3D slice and the distribution of the circles outlined the shape and dimension of the STS (Figure 3B). Scatter graphs were imported as images and embedded with image embedder VGG-16, which was originally proposed by the Visual Geometry Group from the University of Oxford. Thus, generated images representing designed STS were analyzed with for similarity and differences with the software (Orange Version 3.24.1, Orange data mining toolbox in Python, Bioinformatics Lab, University of Ljubljana). Finally, the complete-linkage hierarchical clustering analysis of images was performed (Figure 4).

2.4 | Statistical analysis

Data were analyzed with IBM SPSS Statistics 26.0 (IBM). For each STS, the thickness values of all 3D slices were analyzed with the Shapiro–Wilk test to determine data distribution. Median values together with 25% and 75% quartiles of the individual thickness across each STS were calculated from the excel charts for each shape group and expressed according to the STS orientation.

3 | RESULTS

A set of objective landmarks and standardized steps were established and applied to limit personal error, and 33 soft-tissue substitutes (STS) were designed. STS thickness was measured in a standardized way, following the definition of reference planes and points determined based on the stationary points on the dentition.

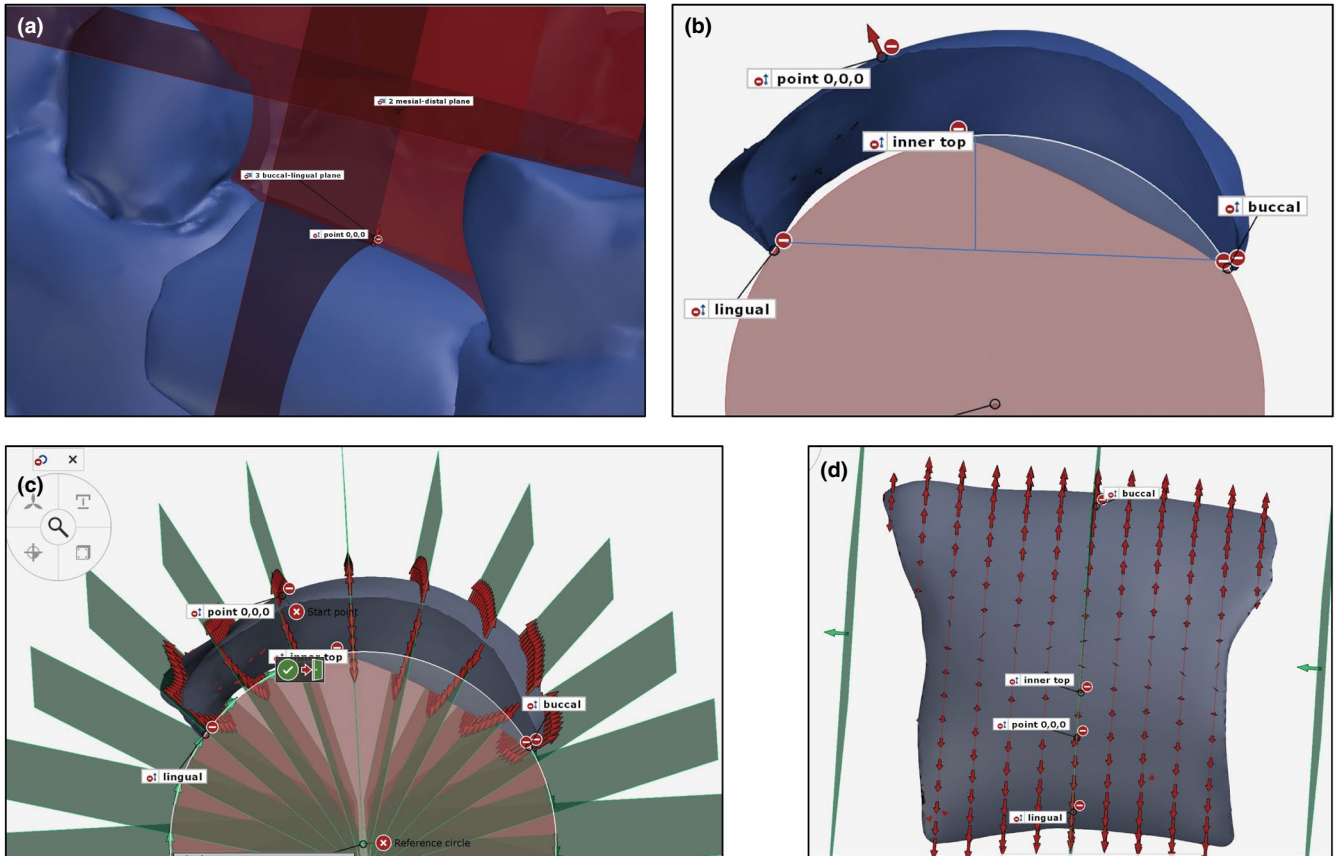


FIGURE 2 Standardized procedure to measure STS thickness. To section the STS into 3D slices where $x = 1$ mm, $y = 1$ mm, and $z = \text{thickness}$, three planes were defined in GOM Inspect: occlusal, mesial–distal, and buccal–lingual plane (a). The circle was designed to fit the inner side of the STS (b) and allow radial sectioning of the STS at 1 mm distance (c). Parallel slicing in mesial–distal and buccal–lingual directions allowed partitioning of the entire STS into a mesh (d)

The thickness values and their position/distribution represented the geometric shape of the STS.

To analyze the size and shape similarities and differences among the designed STS, the 33 scatter graphs were made according to the measurements. With this approach, three-dimensional shapes were decomposed into two-dimensional shapes to simplify comparison across the different STS. The hierarchical clustering data analysis showed the STS shapes separating into two main groups, one corresponding to maxillary and the other to mandibular defects (Figure 4). Further two sub-groups were identified in the maxilla group.

The thickness analysis across the STS indicated a non-normal data distribution. The values, therefore, were calculated as a median (50%), and a range of 25% and 75%. All median STS had the highest thickness in the buccal part, yet presented different shapes. The analysis of the median STS shape for mandible defects ($n = 9$) revealed an oval shape, with the length of 6–8 mm in buccal–lingual and 5–10 mm in mesial–distal direction (Figure 5A). The thickest points (10) ranging from 1.5 mm to 1.9 mm were found in the center of the STS. The thickness gradually decreased from the center toward the edges until 0.1 mm. The highest 25% and 75% values in the center were 1.5 mm (1 point) and 2.0–2.2 mm (5 points), respectively. The median shape of maxilla group 1 ($n = 13$) was square with a maximum length of 10 mm in a buccal–lingual and

7–9 mm in a mesial–distal direction (Figure 5B). The thickest points (12), ranging from 1.5 mm to 1.9 mm, were found in the center of the STS. The thickness gradually decreased toward the edges until 0.006 mm. The highest 25% and 75% values in the center were 1.6–1.8 mm (8 points) and 2.0–2.2 mm (8 points), respectively. The median shape of maxilla group 2 ($n = 11$) was rectangular: longer in the buccal–lingual, with a maximum length of 11 mm, and narrower in the mesial–distal direction with the maximum length of 4–7 mm (Figure 5C). This median STS was the thinnest, with only two thickest points in the center of 1.6 mm. The thickness gradually decreased toward the edges until 0.002 mm. The highest 25% and 75% values in the center were 1.5 mm (1 point) and 1.6–2.2 mm (9 points), respectively.

4 | DISCUSSION

To address the need for an efficient, minimally invasive soft-tissue augmentation approach, a standardized, digital procedure to design optimally fitted soft-tissue substitute (STS) for individual tooth defects, and a mathematical approach to analyze shape and thickness of the STS were developed. This novel approach allowed design of individualized STS for optimal soft-tissue volume augmentation and

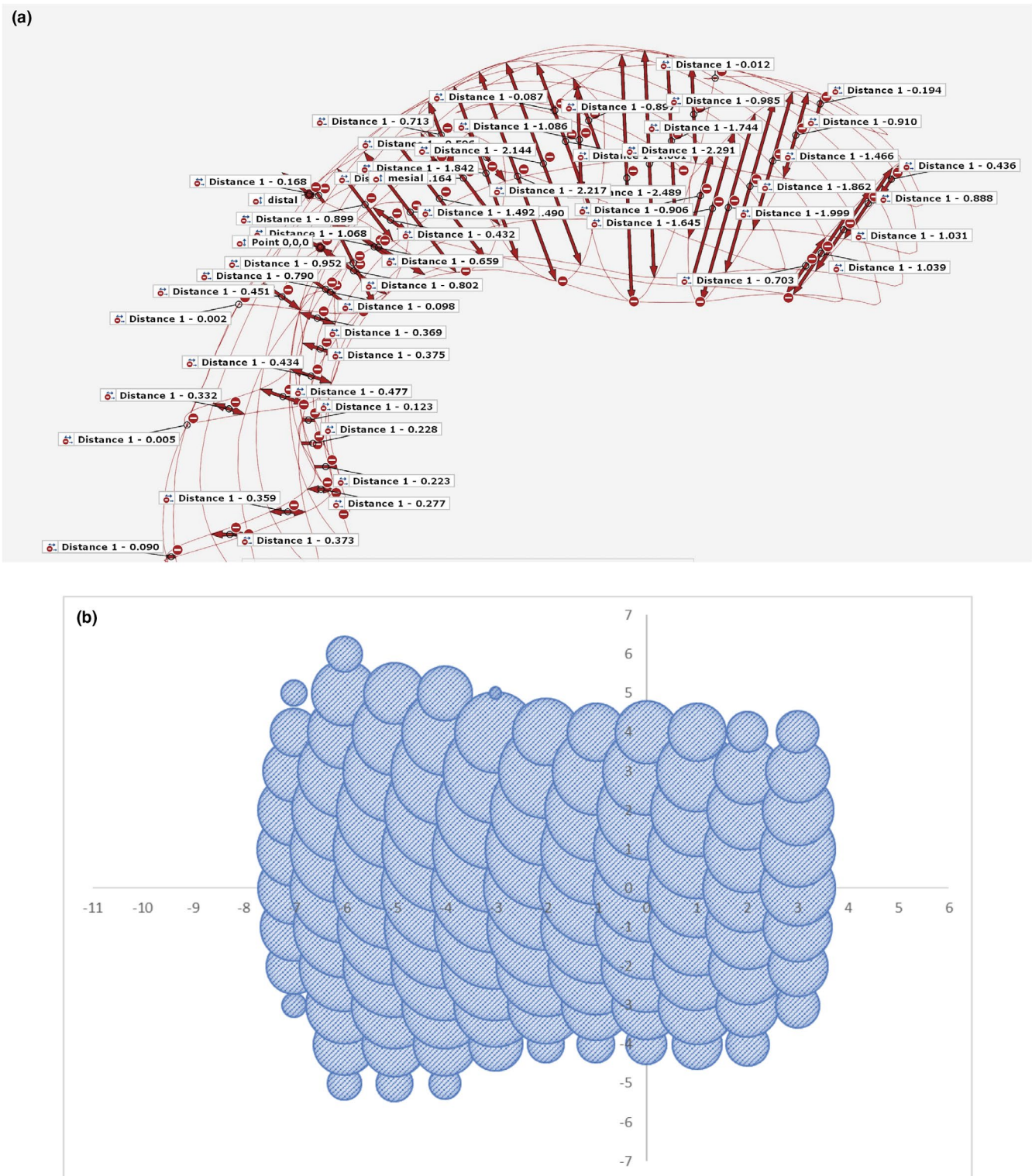


FIGURE 3 Generation of a scattered (“bubble”) graph. Thickness values (z) obtained with GOM Inspect (a) were manually entered into the excel file following the coordinate system to generate a scatter graph (b). The size of each “bubble” corresponds to the thickness value of the 3D slice

identified three average soft-tissue STS shapes for single-tooth defects in the posterior jaw.

Restoration of partially or fully edentulous areas may require both, bone- and soft-tissue augmentation. Sufficient soft tissue

around implants has been correlated with the bone level stability (Di Gianfilippo et al., 2020; D. S. Thoma et al., 2018) and the final esthetic outcomes (Pollini et al., 2020; Tavelli et al., 2020). To optimally restore soft tissues, a harmonious gingival margin

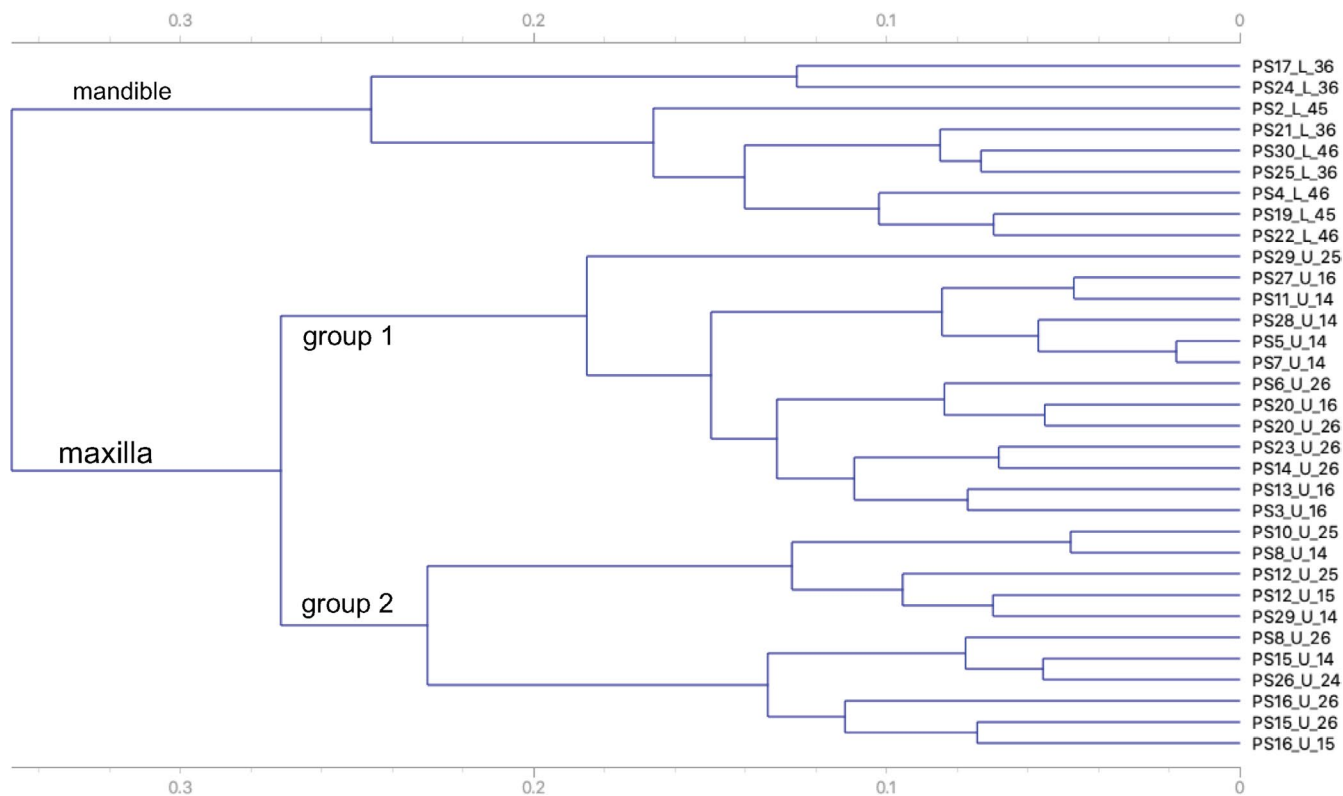


FIGURE 4 Clustering the graph images according to shape. To identify similar shapes, 33 scatter graphs were embedded into images, analyzed and clustered into three groups (Orange): one group for mandible defect shapes, and two groups for maxilla defect shapes. The teeth corresponding to virtually augmented defects are indicated on the right

without height irregularities and an adequate papilla should be created, and a convex contour of the alveolar bone should be followed (Belser et al., 1996). An ideal fit and immobility of the STS are critical for the initial nutrition and oxygenation via plasmatic diffusion until subsequent vascularization (Luo et al., 2020). To overcome disadvantages of the use of CGT for soft-tissue augmentation, different allograft, and xenograft substitutes have been developed and used in clinics. Several reviews evaluated their efficacy. One study found no difference between collagen xenograft matrix (Mucograft, Geistlich), collagen allograft matrix (Alloderm, BioHorizon), and reconstituted collagen matrix (Fibro-Gide, Geistlich) and CTG (Gargallo-Albiol et al., 2019). Two studies showed similar outcome between Alloderm or Fibro-Gide and CTG, yet better performance of CTG than Mucograft (Lissek et al., 2020; Tavelli et al., 2020). A recent randomized controlled clinical trial compared the autogenous sub-epithelial CTG with a volume-stable collagen matrix (VCMX) over a 3 years follow-up time. Differences between the two approaches were negligible and outcomes remained stable (D. S. Thoma et al., 2020). Regardless of the type of reconstruction, an improvement in the soft-tissue volume has been firmly documented. However, while these substitute matrices circumvent second site wounds, decrease surgical time, risk of infections and patient morbidity, the time-consuming shape adaptation of prefabricated over-sized blocks remains an important disadvantage. Two possibilities can be envisaged to circumvent this constrain: production of individualized perfectly fitting STS

and/or production of blocks corresponding to average shapes that would require minimal adaptation prior insertion.

Currently, soft-tissue grafting is solely based on the clinical evaluation, where the operator manually measures the height, width and depth of the defect for subsequent autogenous graft or STS shaping. In contrast, the evaluation of the bone defects had been achieved with CBCT (Guevara Perez et al., 2018; Magat, 2020). A recent study even provided a digital workflow to produce grafts for posterior mandible vertical bone defects (Bartnikowski et al., 2020). To assess the gained soft tissue upon grafting, 2D methods, comprising a periodontal probe (caliper), oral photography and ultrasonic devices, gave way to computerized digital technologies comprising CBCT and 3D lasers (Fons-Badal et al., 2020; Rebele et al., 2014; Ueno et al., 2018). Yet, digital technology has still not found its application in measuring soft-tissue defects. In this proof-of-concept study, STS for posterior single-tooth defects were digitally designed based on conventional impression casts. The basic surgery principles were followed to include the incision lines and extensional ranges in the STS design (Mazzotti et al., 2018; Zucchelli et al., 2018). The inner surface perfectly fitted the irregular defect shape and the outer surface corresponded to the desired ridge contour. Each obtained 3D STS shape was depicted as a series of “bubbles” representing the thickness values of each individual point across the STS. However, the production of individualized STS still demands technical developments with the corresponding clinical implementation. To facilitate the future production of a soft-tissue substitute, which would be better adapted

to the most common defect shapes, a mathematical approach was applied to identify an average STS shape. Given that the thickness values of the STS were not normally distributed, it was not possible to calculate the mathematical average. Another approach was, thus, identified to classify the STS according to their shape. Image embedding was introduced to convert scattered graphs into images, combining a frequently used image embedder VGG-16 based on deep neural networks for image recognition (Vasudevan & Geetha, 2021) followed by the complete-linkage hierarchical clustering. STS images were thus sorted into several groups and a systematic, objective, and comprehensive image classification was achieved.

The final clustering results revealed the distribution of designed STS according to their position in the jaw: mandible or maxilla, validating the use of this approach for the correct STS grouping prior to the average shape analysis. The maxilla STS were longer than mandible STS, in line with their anatomical differences. Maxilla alveolar crest is flatter than mandibular, and a longer STS is needed to cover the defect in the buccal-lingual direction. The thickness of all designed STS was uneven, comprising a thicker central part (1.5–2.2 mm) and an extremely thin margin (less than 0.1 mm). The thickest points corresponded to the standard thickness of sub-epithelial

CTG (1–3 mm) (Amin et al., 2018; Cairo et al., 2017; Lorenzo et al., 2012) but not to the thick volume-stable, yet highly porous substitute collagen block (6–8 mm) (D. S. Thoma et al., 2020; D. S. Thoma et al., 2016; Zeltner et al., 2017). The thickest part in all STS was located on the buccal side, corresponding to the necessary augmentation of the more pronounced loss of the buccal tissues after teeth removal (Araujo et al., 2015; Chappuis et al., 2017).

The stability of the soft tissue after the augmentation procedures has been evaluated in different studies. The application of sub-epithelial CTG at pontic sites had similar resorption as the un-augmented control, reporting loss in pontic height of -0.35 mm (volumetric loss of -4–5 mm³) after 5 years (Sanz-Martin et al., 2016) and -0.2–0.3 mm after 10 years (S. P. Bienz, Sailer, et al., 2017). Soft-tissue augmentation with sub-epithelial CTG on the buccal side at implant sites revealed similar soft-tissue loss with only minimal volumetric and linear differences between treated and untreated sites (-0.4–0.5 mm) after 5 years (S. P. Bienz, Jung, et al., 2017). Several studies compared volumetric changes upon sub-epithelial CTG or collagen soft-tissue substitutes treatments for soft-tissue augmentation at implant sites. The decrease in buccal soft-tissue thickness and volume was -0.1–0.2 mm after 1 year

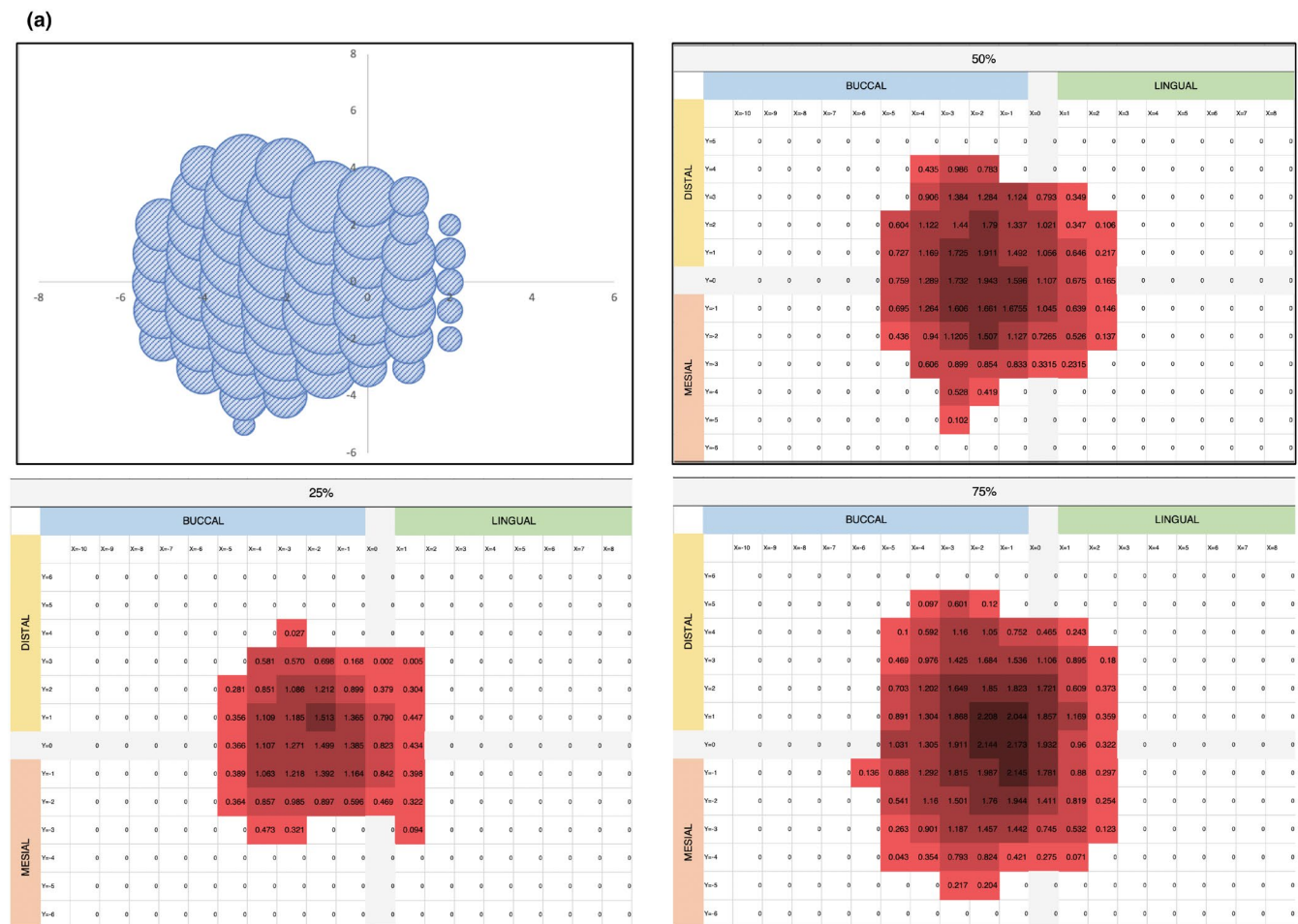


FIGURE 5 Scatter graph outlining the shape, median (50%), 25%, and 75% values depicting thickness across graphs for median mandible, $n = 9$ (a), median maxilla group 1, $n = 13$ (b), and median maxilla group 2, $n = 11$ (c). The intensity of red color corresponds to the thickness ranging from 0.001 mm (lightest shade) to 2.2 mm (darkest shade)

(b)

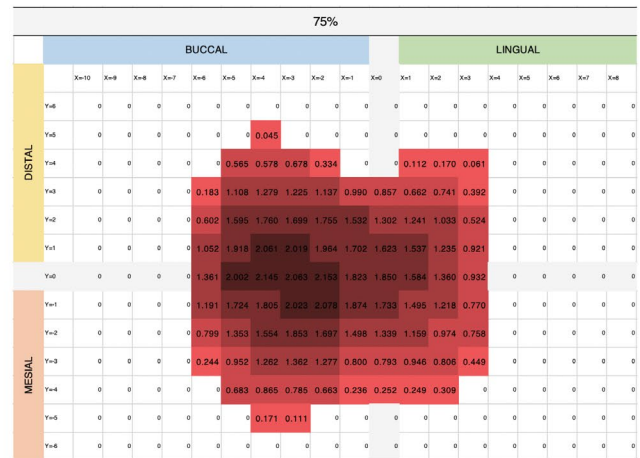
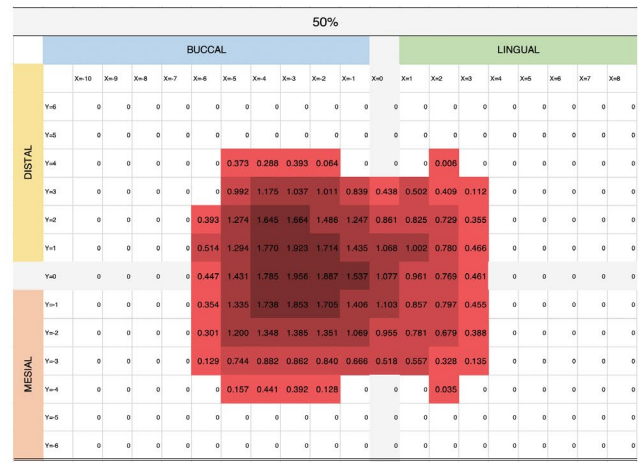
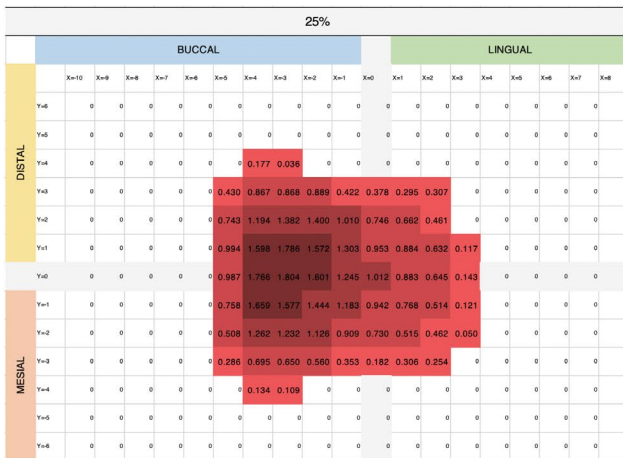
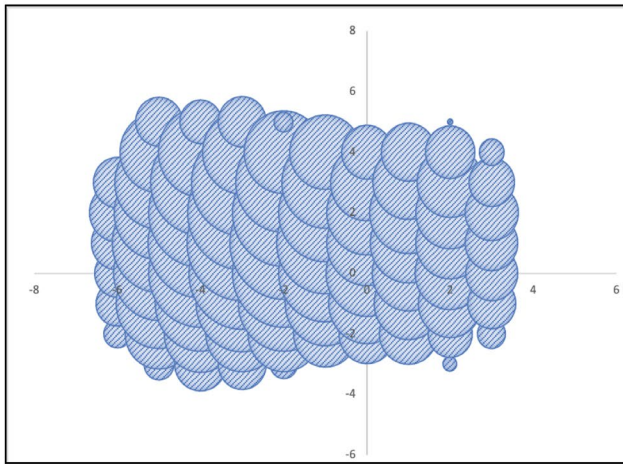


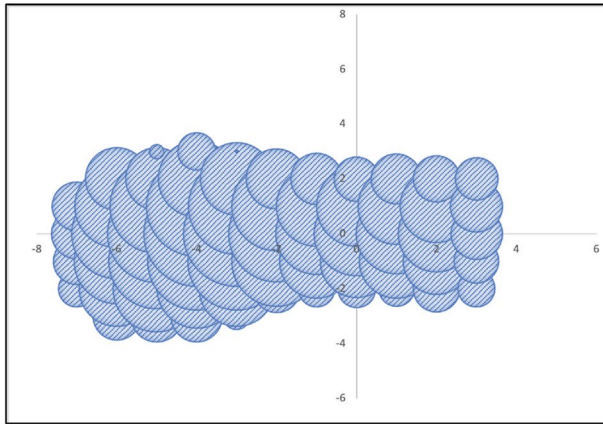
FIGURE 5 (Continues)

(Huber et al., 2018). Another study reported an increase in soft-tissue volume of 0.9 mm for sub-epithelial CTG and of 0.6 mm for the collagen matrix substitute after 3 months (Zeltner et al., 2017). After 3 years, the increase in soft-tissue thickness was 0.8 for sub-epithelial CTG and 0.5 for the collagen matrix. (D. S. Thoma et al., 2020). In the same study, however, a decrease to -0.1 mm for SCTG and -0.2 mm for the collagen matrix was noted in contour, as profilometric changes. These studies suggest scarce documentation of the soft-tissue augmentation procedures and the lack of long-term data. There is an obvious discrepancy in the thickness of CTG and collagen matrices used in different studies. Because CTG is a full and firm piece of connective tissue, usually 1–3 mm thick, thicker STS have been inserted (8 mm) with the intention to compensate for its increased porosity (D. S. Thoma et al., 2020; D. S. Thoma et al., 2017). Whether an over augmentation of the soft-tissue volume is necessary has not been documented. A new approach for a more efficient soft-tissue augmentation and preservation could start by applying the pre-shaped collagen substitute matrices offering better controlled STS remodeling and more volume-stable long-term outcomes. Ultimately, further technological developments, in particular 3D printing, may allow production of optimally fitting, individualized STS (Nesic et al., 2020). In future, both types

of presented STS designs can be manufactured and tested in pre-clinical and clinical studies.

In summary, this study established a standardized digital method to design the geometrical shape of STS to augment volume in single posterior tooth soft-tissue defects and provided a tool to obtain an average shape to reduce STS adaptation time during surgery and upon clinical validation, may allow long-term tissue volume stability. To further validate the approach, future studies should extend the results to the larger number of single posterior defects to achieve a more reliable normalized data distribution, and also include other types of defects, such as double posterior or single/double anterior defects. For the future design of individualized STS shapes, the developed digital procedure could be easily combined with intraoral scanning, avoiding the need for taking and scanning cast impressions, and accelerating the soft-tissue volume augmentation procedure. Moreover, for large defects comprising alveolar bone in addition to soft tissue, a combination of CBCT and intraoral scans may be combined to optimally augment hard and soft-tissue volume. The application of the obtained average shapes for single-tooth soft-tissue defects may result in production of better fitted xenograft or synthetic STS blocks. Both approaches would reduce clinical time, patient discomfort and potentially improve soft-tissue volume augmentation.

(c)



		50%															
		BUCCAL										LINGUAL					
		X=9	X=8	X=7	X=6	X=5	X=4	X=3	X=2	X=1	X=0	X=1	X=2	X=3	X=4	X=5	X=6
DISTAL	Y=4	0	0	0	0	0	0	0	0	0	0	0	0	0	0	0	0
	Y=3	0	0	0	0	0.034	0.207	0.002	0	0	0	0	0	0	0	0	0
	Y=2	0	0	0	0.564	0.553	0.818	0.745	0.518	0.377	0.287	0.363	0.313	0.262	0	0	0
	Y=1	0	0	0.347	0.977	1.23	1.403	1.307	1.114	0.915	0.906	0.836	0.738	0.386	0	0	0
MESIAL	Y=0	0	0	0.362	1.15	1.347	1.568	1.564	1.296	0.933	1.004	0.919	0.823	0.376	0	0	0
	Y=1	0	0	0.308	1.016	1.294	1.34	1.349	1.136	0.771	0.749	0.78	0.627	0.285	0	0	0
	Y=2	0	0	0.194	0.795	1.052	0.896	0.805	0.323	0.197	0.209	0.189	0.307	0.198	0	0	0
	Y=3	0	0	0	0.331	0.384	0.382	0.107	0	0	0	0	0	0	0	0	0
Y=4	0	0	0	0	0	0	0	0	0	0	0	0	0	0	0	0	

		25%															
		BUCCAL										LINGUAL					
		X=9	X=8	X=7	X=6	X=5	X=4	X=3	X=2	X=1	X=0	X=1	X=2	X=3	X=4	X=5	X=6
DISTAL	Y=4	0	0	0	0	0	0	0	0	0	0	0	0	0	0	0	0
	Y=3	0	0	0	0	0	0	0	0	0	0	0	0	0	0	0	0
	Y=2	0	0	0	0.191	0.466	0.492	0.570	0.359	0.217	0.182	0.261	0.245	0	0	0	0
	Y=1	0	0	0	0.716	0.924	1.015	1.140	0.971	0.671	0.626	0.666	0.652	0.157	0	0	0
MESIAL	Y=0	0	0	0	0.899	1.327	1.538	1.412	1.150	0.833	0.804	0.812	0.687	0.147	0	0	0
	Y=1	0	0	0	0.676	0.953	1.096	1.077	0.904	0.604	0.634	0.667	0.589	0	0	0	0
	Y=2	0	0	0	0.447	0.558	0.702	0.495	0.077	0	0.006	0.118	0.165	0	0	0	0
	Y=3	0	0	0	0.166	0.332	0.239	0	0	0	0	0	0	0	0	0	0
Y=4	0	0	0	0	0	0	0	0	0	0	0	0	0	0	0	0	

		75%															
		BUCCAL										LINGUAL					
		X=9	X=8	X=7	X=6	X=5	X=4	X=3	X=2	X=1	X=0	X=1	X=2	X=3	X=4	X=5	X=6
DISTAL	Y=4	0	0	0	0	0	0	0	0	0	0	0	0	0	0	0	0
	Y=3	0	0	0	0	0.22	0.419	0.378	0.21	0	0	0	0	0	0	0.126	0
	Y=2	0	0.048	0.626	0.886	0.842	1.136	0.928	0.819	0.837	0.728	0.526	0.437	0.37	0.234	0	0
	Y=1	0	0.622	1.115	1.437	1.454	1.631	1.457	1.208	1.035	1.083	0.976	0.820	0.729	0.609	0	0
MESIAL	Y=0	0	0.813	1.175	1.710	2.134	2.157	1.844	1.446	1.298	1.164	1.106	1.086	0.953	0.841	0	0
	Y=1	0	0.754	1.113	1.502	1.852	1.574	1.181	1.146	1.053	1.140	0.979	0.706	0.511	0	0	
	Y=2	0	0.581	0.930	1.135	1.261	1.149	0.955	0.690	0.532	0.250	0.369	0.348	0.329	0.205	0	0
	Y=3	0	0.015	0.472	0.519	0.777	0.726	0.374	0	0	0	0	0	0	0	0	0
Y=4	0	0	0	0	0	0.089	0	0	0	0	0	0	0	0	0	0	

FIGURE 5 (Continues)

ACKNOWLEDGMENTS

This study was funded by Geistlich Pharma AG. The authors are grateful to Dr Philippe Mojon for his valuable advice in statistical analysis. The authors declare no potential conflicts of interest with respect to the authorship and/or publication of this article. Open Access funding provided by Universite de Geneve.

CONFLICTS OF INTEREST

The authors declare no potential conflicts of interest with respect to the authorship and/or publication of this article. Birgit Schäfer is an employee of Geistlich Pharma AG.

AUTHOR CONTRIBUTIONS

Yue Sun: Data curation (equal); Formal analysis (equal); Investigation (equal); Methodology (equal); Writing-original draft (equal). **Tao Yu:** Data curation (equal); Formal analysis (equal); Investigation (equal); Methodology (equal); Validation (equal); Writing-original draft (equal). **Malin Stranding:** Conceptualization (equal); Data curation (supporting); Investigation (equal); Methodology (supporting); Validation (equal); Writing-original draft (equal). **Birgit M Schaefer:** Conceptualization (equal); Methodology (supporting); Supervision (supporting); Validation (supporting); Writing-review & editing (equal). **Irena Sailer:** Conceptualization (equal); Funding acquisition (lead); Methodology (supporting); Project administration (supporting); Supervision (supporting); Writing-review & editing (equal). **Dobriła Nesić:** Conceptualization

(supporting); Formal analysis (supporting); Funding acquisition (supporting); Project administration (lead); Supervision (lead); Writing-original draft (lead); Writing-review & editing (equal).

DATA AVAILABILITY STATEMENT

The data that support the findings of this study are available from the corresponding author upon reasonable request.

ORCID

- Yue Sun <https://orcid.org/0000-0001-8452-5944>
- Irena Sailer <https://orcid.org/0000-0002-4537-7624>
- Dobriła Nesić <https://orcid.org/0000-0003-1609-9255>

REFERENCES

Ackali, A., Trullenque-Eriksson, A., Sun, C., Petrie, A., Nibali, L., & Donos, N. (2017). What is the effect of soft tissue thickness on crestal bone loss around dental implants? A systematic review. *Clinical Oral Implants Research*, 28(9), 1046–1053. <https://doi.org/10.1111/clr.12916>

Amin, P. N., Bissada, N. F., Ricchetti, P. A., Silva, A. P. B., & Demko, C. A. (2018). Tuberosity versus palatal donor sites for soft tissue grafting: A split-mouth clinical study. *Quintessence International*, 49(7), 589–598. <https://doi.org/10.3290/j.qi.a40510>

Araujo, M. G., Silva, C. O., Misawa, M., & Sukekava, F. (2015). Alveolar socket healing: What can we learn? *Periodontology* 2000, 68(1), 122–134. <https://doi.org/10.1111/prd.12082>

- Bartnikowski, M., Vaquette, C., & Ivanovski, S. (2020). Workflow for highly porous resorbable custom 3D printed scaffolds using medical grade polymer for large volume alveolar bone regeneration. *Clinical Oral Implants Research*, 31(5), 431–441. <https://doi.org/10.1111/clr.13579>
- Bassetti, R. G., Stahli, A., Bassetti, M. A., & Sculean, A. (2016). Soft tissue augmentation procedures at second-stage surgery: A systematic review. *Clinical Oral Investigations*, 20(7), 1369–1387. <https://doi.org/10.1007/s00784-016-1815-2>
- Batista, M. J., Rihs, L. B., & Sousa Mda, L. (2012). Risk indicators for tooth loss in adult workers. *Brazilian Oral Research*, 26(5), 390–396. <https://doi.org/10.1590/s1806-83242012000500003>
- Belser, U. C., Bernard, J. P., & Buser, D. (1996). Implant-supported restorations in the anterior region: Prosthetic considerations. *Practical Periodontics and Aesthetic Dentistry: PPAD*, 8(9), 875–883. quiz 884.
- Benninger, B., Andrews, K., & Carter, W. (2012). Clinical measurements of hard palate and implications for subepithelial connective tissue grafts with suggestions for palatal nomenclature. *Journal of Oral and Maxillofacial Surgery*, 70(1), 149–153. <https://doi.org/10.1016/j.joms.2011.03.066>
- Bienz, S. P., Jung, R. E., Sapata, V. M., Hämmerle, C. H. F., Hüsler, J. J., & Thoma, D. S. (2017). Volumetric changes and peri-implant health at implant sites with or without soft tissue grafting in the esthetic zone, a retrospective case-control study with a 5-year follow-up. *Clinical Oral Implants Research*, 28(11), 1459–1465. <https://doi.org/10.1111/clr.13013>
- Bienz, S. P., Sailer, I., Sanz-Martin, I., Jung, R. E., Hammerle, C. H., & Thoma, D. S. (2017). Volumetric changes at pontic sites with or without soft tissue grafting: A controlled clinical study with a 10-year follow-up. *Journal of Clinical Periodontology*, 44(2), 178–184. <https://doi.org/10.1111/jcpe.12651>
- Cairo, F., Barbato, L., Tonelli, P., Batalocco, G., Pagavino, G., & Nieri, M. (2017). Xenogeneic collagen matrix versus connective tissue graft for buccal soft tissue augmentation at implant site. A randomized, controlled clinical trial. *Journal of Clinical Periodontology*, 44(7), 769–776. <https://doi.org/10.1111/jcpe.12750>
- Chappuis, V., Araujo, M. G., & Buser, D. (2017). Clinical relevance of dimensional bone and soft tissue alterations post-extraction in esthetic sites. *Periodontology 2000*, 73(1), 73–83. <https://doi.org/10.1111/prd.12167>
- De Bruyckere, T., Eghbali, A., Younes, F., De Bruyn, H., & Cosyn, J. (2015). Horizontal stability of connective tissue grafts at the buccal aspect of single implants: A 1-year prospective case series. *Journal of Clinical Periodontology*, 42(9), 876–882. <https://doi.org/10.1111/jcpe.12448>
- Di Gianfilippo, R., Valente, N. A., Toti, P., Wang, H. L., & Barone, A. (2020). Influence of implant mucosal thickness on early bone loss: A systematic review with meta-analysis. *Journal of Periodontal & Implant Science*, 50(4), 209–225. <https://doi.org/10.5051/jpis.1904440222>
- Dye, B. A., Weatherspoon, D. J., & Lopez Mitnik, G. (2019). Tooth loss among older adults according to poverty status in the United States from 1999 through 2004 and 2009 through 2014. *The Journal of the American Dental Association*, 150(1), 9–23. <https://doi.org/10.1016/j.adaj.2018.09.010>
- Fons-Badal, C., Alonso Perez-Barquero, J., Martinez-Martinez, N., Faus-Lopez, J., Fons-Font, A., & Agustin-Panadero, R. (2020). A novel, fully digital approach to quantifying volume gain after soft tissue graft surgery. A pilot study. *Journal of Clinical Periodontology*, 47(5), 614–620. <https://doi.org/10.1111/jcpe.13235>
- Gargallo-Albiol, J., Barootchi, S., Tavelli, L., & Wang, H. L. (2019). Efficacy of xenogeneic collagen matrix to augment peri-implant soft tissue thickness compared to autogenous connective tissue graft: A systematic review and meta-analysis. *International Journal of Oral and Maxillofacial Implants*, 34(5), 1059–1069. <https://doi.org/10.11607/jomi.7497>
- Gobbato, L., Avila Ortiz, G., Sohrabi, K., Wang, C., & Karimbux, N. (2013). The effect of keratinized mucosa width on peri-implant health: A systematic review. *The International Journal of Oral & Maxillofacial Implants*, 28(6), 1536–1545. <https://doi.org/10.11607/jomi.3244>
- Guevara Perez, S. V., de la Rosa Castolo, G., Thollon, L., & Behr, M. (2018). A 3D characterization method of geometric variation in edentulous mandibles. *Morphologie*, 102(339), 255–262. <https://doi.org/10.1016/j.morpho.2018.08.001>
- Huber, S., Zeltner, M., Hämmerle, C. H. F., Jung, R. E., & Thoma, D. S. (2018). Non-interventional 1-year follow-up study of peri-implant soft tissues following previous soft tissue augmentation and crown insertion in single-tooth gaps. *Journal of Clinical Periodontology*, 45(4), 504–512. <https://doi.org/10.1111/jcpe.12865>
- Lin, H. C., Corbet, E. F., Lo, E. C., & Zhang, H. G. (2001). Tooth loss, occluding pairs, and prosthetic status of Chinese adults. *Journal of Dental Research*, 80(5), 1491–1495. <https://doi.org/10.1177/00220345010800052101>
- Lissek, M., Boeker, M., & Happe, A. (2020). How thick is the oral mucosa around implants after augmentation with different materials: A systematic review of the effectiveness of substitute matrices in comparison to connective tissue grafts. *International Journal of Molecular Sciences*, 21(14), 5043. <https://doi.org/10.3390/ijms21145043>
- Lorenzo, R., Garcia, V., Orsini, M., Martin, C., & Sanz, M. (2012). Clinical efficacy of a xenogeneic collagen matrix in augmenting keratinized mucosa around implants: A randomized controlled prospective clinical trial. *Clinical Oral Implants Research*, 23(3), 316–324. <https://doi.org/10.1111/j.1600-0501.2011.02260.x>
- Luo, R. M., Chvartzaid, D., Kim, S. W., & Portnof, J. E. (2020). Soft-tissue grafting solutions. *Dental Clinics of North America*, 64(2), 435–451. <https://doi.org/10.1016/j.cden.2019.12.008>
- Magat, G. (2020). Radiomorphometric analysis of edentulous posterior mandibular ridges in the first molar region: A cone-beam computed tomography study. *Journal of Periodontal & Implant Science*, 50(1), 28–37. <https://doi.org/10.5051/jpis.2020.50.1.28>
- Mazzotti, C., Stefanini, M., Felice, P., Bentivogli, V., Mounssif, I., & Zucchelli, G. (2018). Soft-tissue dehiscence coverage at peri-implant sites. *Periodontology 2000*, 77(1), 256–272. <https://doi.org/10.1111/prd.12220>
- Muller, F., Naharro, M., & Carlsson, G. E. (2007). What are the prevalence and incidence of tooth loss in the adult and elderly population in Europe? *Clinical Oral Implants Research*, 18(Suppl. 3), 2–14. <https://doi.org/10.1111/j.1600-0501.2007.01459.x>
- Nesic, D., Schaefer, B. M., Sun, Y., Saulacic, N., & Sailer, I. (2020). 3D Printing approach in dentistry: The future for personalized oral soft tissue regeneration. *Journal of Clinical Medicine*, 9(7), 2238. <https://doi.org/10.3390/jcm9072238>
- Pollini, A., Morton, D., Arunyanak, S. P., Harris, B. T., & Lin, W. S. (2020). Evaluation of esthetic parameters related to a single implant restoration by laypeople and dentists. *Journal of Prosthetic Dentistry*, 124(1), 94–99. <https://doi.org/10.1016/j.prosdent.2019.08.017>
- Rebele, S. F., Zuhr, O., Schneider, D., Jung, R. E., & Hurzeler, M. B. (2014). Tunnel technique with connective tissue graft versus coronally advanced flap with enamel matrix derivative for root coverage: a RCT using 3D digital measuring methods. Part II. Volumetric studies on healing dynamics and gingival dimensions. *Journal of Clinical Periodontology*, 41(6), 593–603. <https://doi.org/10.1111/jcpe.12254>
- Sanz, M., Lorenzo, R., Aranda, J. J., Martin, C., & Orsini, M. (2009). Clinical evaluation of a new collagen matrix (Mucograft prototype) to enhance the width of keratinized tissue in patients with fixed prosthetic restorations: A randomized prospective clinical trial. *Journal of Clinical Periodontology*, 36(10), 868–876. <https://doi.org/10.1111/j.1600-051X.2009.01460.x>
- Sanz-Martin, I., Sailer, I., Hammerle, C. H., & Thoma, D. S. (2016). Soft tissue stability and volumetric changes after 5 years in pontic

- sites with or without soft tissue grafting: A retrospective cohort study. *Clinical Oral Implants Research*, 27(8), 969–974. <https://doi.org/10.1111/clr.12743>
- Sculean, A., Romanos, G., Schwarz, F., Ramanauskaitė, A., Keeve, P. L., Khoury, F., Koo, K. T., & Cosgarea, R. (2019). Soft-tissue management as part of the surgical treatment of periimplantitis: A narrative review. *Implant Dentistry*, 28(2), 210–216. <https://doi.org/10.1097/ID.0000000000000870>
- Tavelli, L., Barootchi, S., Avila-Ortiz, G., Urban, I. A., Giannobile, W. V., & Wang, H. L. (2020). Peri-implant soft tissue phenotype modification and its impact on peri-implant health: A systematic review and network meta-analysis. *Journal of Periodontology*, <https://doi.org/10.1002/JPER.19-0716>
- Thoma, D. S., Buranawat, B., Hammerle, C. H., Held, U., & Jung, R. E. (2014). Efficacy of soft tissue augmentation around dental implants and in partially edentulous areas: A systematic review. *Journal of Clinical Periodontology*, 41(Suppl. 15), S77–S91. <https://doi.org/10.1111/jcpe.12220>
- Thoma, D. S., Gasser, T. J. W., Jung, R. E., & Hammerle, C. H. F. (2020). Randomized controlled clinical trial comparing implant sites augmented with a volume-stable collagen matrix or an autogenous connective tissue graft: 3-Year data after insertion of reconstructions. *Journal of Clinical Periodontology*, 47(5), 630–639. <https://doi.org/10.1111/jcpe.13271>
- Thoma, D. S., Muhlemann, S., & Jung, R. E. (2014). Critical soft-tissue dimensions with dental implants and treatment concepts. *Periodontology 2000*, 66(1), 106–118. <https://doi.org/10.1111/prd.12045>
- Thoma, D. S., Naenni, N., Benic, G. I., Hammerle, C. H., & Jung, R. E. (2017). Soft tissue volume augmentation at dental implant sites using a volume stable three-dimensional collagen matrix-histological outcomes of a preclinical study. *Journal of Clinical Periodontology*, 44(2), 185–194. <https://doi.org/10.1111/jcpe.12635>
- Thoma, D. S., Naenni, N., Figuero, E., Hämmerle, C. H. F., Schwarz, F., Jung, R. E., & Sanz Sanchez, I. (2018). Effects of soft tissue augmentation procedures on peri-implant health or disease: A systematic review and meta-analysis. *Clinical Oral Implants Research*, 29(Suppl. 15), 32–49. <https://doi.org/10.1111/clr.13114>
- Thoma, D. S., Zeltner, M., Hilbe, M., Hammerle, C. H., Husler, J., & Jung, R. E. (2016). Randomized controlled clinical study evaluating effectiveness and safety of a volume-stable collagen matrix compared to autogenous connective tissue grafts for soft tissue augmentation at implant sites. *Journal of Clinical Periodontology*, 43(10), 874–885. <https://doi.org/10.1111/jcpe.12588>
- Toledano, M., Toledano-Osorio, M., Carrasco-Carmona, A., Vallecillo, C., Lynch, C. D., Osorio, M. T., & Osorio, R. (2020). State of the art on biomaterials for soft tissue augmentation in the oral cavity. Part I: Natural polymers-based biomaterials. *Polymers (Basel)*, 12(8), 1850. <https://doi.org/10.3390/polym12081850>
- Ueno, D., Kobayashi, M., Tanaka, K., Watanabe, T., Nakamura, T., Ueda, K., & Nagano, T. (2018). Measurement accuracy of alveolar soft tissue contour using a laboratory laser scanner. *Odontology*, 106(2), 202–207. <https://doi.org/10.1007/s10266-017-0315-4>
- Van der Weijden, F., Dell'Acqua, F., & Slot, D. E. (2009). Alveolar bone dimensional changes of post-extraction sockets in humans: A systematic review. *Journal of Clinical Periodontology*, 36(12), 1048–1058. <https://doi.org/10.1111/j.1600-051X.2009.01482.x>
- Vasudevan, S., Sarobin, V., & Geetha, S. (2021). Image-based recommendation engine using VGG model. In Springer (Ed.). *Advances in communication and computational technology*. (Vol. 668).
- Wolff, J., Farre-Guasch, E., Sandor, G. K., Gibbs, S., Jager, D. J., & Forouzanfar, T. (2016). Soft tissue augmentation techniques and materials used in the oral cavity: An overview. *Implant Dentistry*, 25(3), 427–434. <https://doi.org/10.1097/ID.0000000000000385>
- Zeltner, M., Jung, R. E., Hammerle, C. H., Husler, J., & Thoma, D. S. (2017). Randomized controlled clinical study comparing a volume-stable collagen matrix to autogenous connective tissue grafts for soft tissue augmentation at implant sites: Linear volumetric soft tissue changes up to 3 months. *Journal of Clinical Periodontology*, 44(4), 446–453. <https://doi.org/10.1111/jcpe.12697>
- Zucchelli, G., Tavelli, L., Ravidà, A., Stefanini, M., Suarez-Lopez Del Amo, F., & Wang, H. L. (2018). Influence of tooth location on coronally advanced flap procedures for root coverage. *Journal of Periodontology*, 89(12), 1428–1441. <https://doi.org/10.1002/JPER.18-0201>

How to cite this article: Sun, Y., Yu, T., Strasding, M., Liu, X., Burkhardt, F., Schäfer, B., Sailer, I., & Nestic, D. (2021). Design of customized soft-tissue substitutes for posterior single-tooth defects: A proof-of-concept in-vitro study. *Clinical Oral Implants Research*, 32, 1263–1273. <https://doi.org/10.1111/clr.13831>